Field-assisted spin-polarized electron transport through a single quantum well with spin–orbit coupling*

Ding Xiu-Huan(丁秀欢)[a)b)], Zhang Cun-Xi(张存喜)[c)†], Wang Rui(王 瑞)[c)], Zhou Yun-Qing(周运清)[c)], and Kong Ling-Min(孔令民)[c)]

[a)] *Department of Mathematics, Zhejiang Ocean University, Zhoushan* 316000, *China*

[b)] *Key Laboratory of Symbolic Computation and Knowledge Engineering of Ministry of Education, Jilin University, Changchun* 130012, *China*

[c)] *Department of Physics, Zhejiang Ocean University, Zhoushan* 316000, *China*

(Received 7 November 2011; revised manuscript received 23 November 2011)

We have investigated theoretically the field-driven electron transport through a single-quantum-well semiconductor heterostructure with spin–orbit coupling. The splitting of the asymmetric Fano-type resonance peaks due to the Dresselhaus spin–orbit coupling is found to be highly sensitive to the direction of the incident electron. The splitting of the Fano-type resonance induces the spin-polarization dependent electron current. The location and the line shape of the Fano-type resonance can be controlled by adjusting the energy and the direction of the incident electron, the oscillation frequency, and the amplitude of the external field. These interesting features may be used to devise tunable spin filters and realize pure spin transmission currents.

Keywords: Fano resonance, Floquet channel, spin–orbit coupling

PACS: 73.23.–b, 72.25.Dc, 73.63.Hs **DOI:** 10.1088/1674-1056/21/3/037302

1. Introduction

Recently, spin-dependent quantum transport has become one of the most evolving fields in semiconductor science due to its potential extensive applications. It may provide a controllable way to orient, manipulate, and detect spins in semiconductors by electrical means, and it is an indispensable basis guiding the designs of spintronic devices, such as the spin filter. A natural way to control the spin orientation in experiment is the injection of spin-polarized carriers from magnetic materials. Although significant progress hasbeen made in experimental and theoretical investigations of the spin-polarized transport in magnetic tunneling junctions (see Refs. [1] and [2] and references therein), the small spin injection efficiency from a ferromagnetic metallic contact into a semiconductor due to the conductivity mismatch[3] is still a fundamental obstacle. Rashba showed that this problem could be resolved by using a tunneling contact at the metal–semiconductor interface.[4] The achievement of spin filtering by means of the intrinsic spin-dependent effects in semiconductors is highly desirable and also very intriguing from the viewpoint of fundamental science. Voskoboynikov *et al.*[5,6] proposed that an asymmetric nonmagnetic semiconductor barrier itself could serve as a spin filter. The effect of spin-dependent tunneling in nonmagnetic semiconductor heterostructures was supposed to be applicable for the spin injection[7–10] and the detection of spin-polarized carriers.[11,12] Devices based on the spin-dependent tunneling were suggested to be utilized as components of the spin field-effect transistor.[11] Recently, Yassievich *et al.*[13,14] have demonstrated that in the heterostructures made of nonmagnetic semiconductor material with bulk inversion asymmetry, the k^3 Dresselhaus spin–orbit interaction, which couples the spin states and the space motion of the conduction electrons, could lead to a clear spin-dependent splitting of the transmission resonances through a double-barrier

*Project supported by the National Natural Science Foundation of China (Grant Nos. 11147173 and 61106052), the Zhejiang Education Department, China (Grant No. Y201018926 and Y200908466), the Basic Research Foundation of Jilin University, China (Grant No. 93K172011K02), the Basic Research Foundation of Zhejiang Ocean University, the Nature Science Foundation of Zhejiang Province, China (Grant No. 1047172), and the Open Foundation from Ocean Fishery Science and Technology in the Most Important Subjects of Zhejiang, China(No. 20110105).

†Corresponding author. E-mail: cunxizhang@yahoo.com.cn

© 2012 Chinese Physical Society and IOP Publishing Ltd

system. The applied oscillating field in the spin–orbit coupling region provides a feasible scheme for controlling the spin-dependent transport through the system.[15−19] In the system with a periodically driven field, the quantum interference between a bound state and the band continuum leads to the appearance of the asymmetric Fano-type resonance.[15−19] In order to acquire an obvious splitting of the asymmetric Fano-type resonance peaks due to the Dresselhaus spin–orbit coupling, $k_{||}$ (the wave vector of the incident electron parallel to the well) is fixed to a relatively large value of 0.1 nm^{-1}[15−18] or 0.2 nm^{-1}.[19] From the experimental and the theoretical points of view, $k_{||}$ should be variable. In this work, on the basis of Ref. [15], we investigate how to affect the splitting of the asymmetric Fano-type resonance peaks due to the Dresselhaus spin–orbit coupling by changing the incident angle of the electron. The results demonstrate that the splitting of the asymmetric Fano-type resonance peaks due to the Dresselhaus spin–orbit coupling is highly sensitive to the direction of the incident electron. It may be used to devise tunable spin filters and realize pure spin transmission currents by controlling the external parameters.

2. Model and formalism

We consider the transmission of a single electron with incident wave vector $\left(k_{||} = k\sin\theta, k_z = k\cos\theta\right)$ above a single potential well made of three layers of semiconductors InP/GaSb/InP, where k is the wave vector of the incident electron, k_z is the wave vector normal to the well plane pointing along the direction of transmission, and $\theta \in (-\pi/2, \pi/2)$ is the angle between k_z and k. One applied oscillating field is confined in the well formed by a layer of narrow band gap semiconductor (GaSb) with a large Dresselhaus spin–orbit coupling. The electron passes three regions I, II, and III respectively from left to right (see Fig. 1). The effective masses of electron outside and inside the well are μ_1 and μ_2, respectively. The oscillating potential is

$$V(z,t) = \begin{cases} 0, & \text{other}, \\ -V_0 + V_1\cos(\omega t), & -a/2 \leqslant z \leqslant a/2, \end{cases} \tag{1}$$

where V_0 is the static well depth, V_1 and ω denote the amplitude and the frequency of the applied oscillating field, respectively. We assume the temperature to be low enough so that the electron–phonon interactions can be neglected. Thus the electron motion in each layer of the semiconductor structure may be described by a time-dependent Schrödinger equation

$$\mathrm{i}\,\hbar\frac{\partial}{\partial t}\Phi(z,s,t) = \hat{H}\Phi(z,s,t), \tag{2}$$

$$\hat{H} = -\frac{\hbar^2}{2\mu}\frac{\partial^2}{\partial z^2} + \frac{\hbar^2 k_{||}^2}{2\mu} + V(z,t) + \hat{H}_{\mathrm{D}}, \tag{3}$$

where μ is the effective electron mass, and $\hat{H}_{\mathrm{D}}$ denotes the spin-dependent Dresselhaus term in the Zinc-blende structure semiconductor.[20] Assume that the kinetic energy of the incidence electron is substantially smaller than the well depth V_0, then the Dresselhaus term $\hat{H}_{\mathrm{D}}$ is simplified to[13,14]

$$\hat{H}_{\mathrm{D}} = \begin{cases} 0, & \text{other}, \\ \gamma\left(\hat{\sigma}_x k_x - \hat{\sigma}_y k_y\right)\dfrac{\partial^2}{\partial z^2}, & -a/2 \leqslant z \leqslant a/2, \end{cases} \tag{4}$$

where γ is a material constant describing the strength of the spin–orbit coupling, and $\hat{\sigma}_i$ $(i = x, y)$ is the Pauli matrix. For the InP/GaSb/InP quantum structure, γ in the well is much larger than that outside the well, so we have assumed that $\gamma \approx 0$ outside the well. Inserting $\Phi(z,s,t) = \psi(z,t)\chi_s$ with χ_s being the spin wave function into Schrödinger Eq. (2), we obtain

$$\chi_{\pm} = \frac{1}{\sqrt{2}}\begin{pmatrix} 1 \\ \mp\,\mathrm{e}^{-\,\mathrm{i}\,\varphi} \end{pmatrix}, \tag{5}$$

where $\chi_{\pm}$ are two pure spinor states, and φ denotes the polar angle of the wave vector $\boldsymbol{k}_{\parallel} = \left(k_{\parallel}\cos\varphi, k_{\parallel}\sin\varphi\right)$ in the xy plane. The orientations of electron spin $\boldsymbol{s}_{\pm}(\boldsymbol{k}_{||}) = \chi_{\pm}^{+}\hat{\sigma}\chi_{\pm} = (\mp\cos\varphi, \pm\sin\varphi, 0)$ corresponding to the eigenstates $\chi_{\pm}$ depend on the direction of wave vector $\boldsymbol{k}_{\parallel}$. In equilibrium, the momentum distribution of the incident electrons is isotropic in the xy plane, and therefore the average spin of the transmitted electrons vanishes.[13] In order to obtain a net spin polarization in the transmitted electrons, we consider the case that the in-plane wave vector of the incident electron is along a fixed direction, for example $\varphi = 0$, which may be achieved by applying an electric field along the $-x$ direction. In the spin subspace, the Hamiltonian reduces to

$$\hat{H}_{\pm} = \chi_{\pm}^{+}\hat{H}\chi_{\pm} = -\frac{\hbar^2}{2\mu_{\pm}}\frac{\partial^2}{\partial z^2} + \frac{\hbar^2 k_{\parallel}^2}{2\mu_2} + V(z,t), \tag{6}$$

where the modified effective mass of electron is given by

$$\mu_{\pm} = \mu_2\left(1 \pm \gamma 2\mu_2 k_{||}/\hbar^2\right)^{-1}. \tag{7}$$

Although the modification to the effective mass of electron is very small, it plays an important role in

the generation of the asymmetric Fano resonance peak splitting.

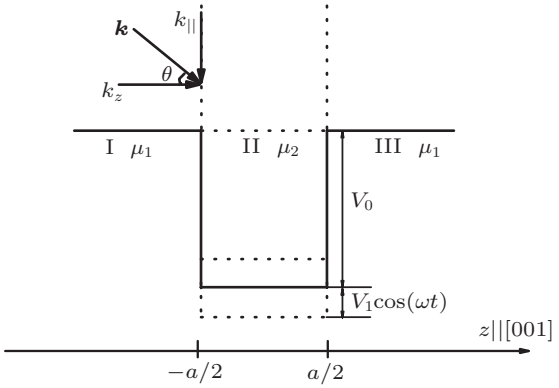


Fig. 1. Schematic diagram of the model for electron transmission through (001)-grown single well structure under applied oscillation field $V_1\cos(\omega t)$.

Using the Floquet theory,[21−23] we obtain the wave function inside the potential well[15]

$$\begin{aligned}&\Phi_{\pm}^{\mathrm{II}}(z,t)\\ &= \chi_{\pm}\sum_{n=-\infty}^{+\infty}\sum_{m=-\infty}^{+\infty}[a_m^{\pm}\,\mathrm{e}^{\mathrm{i}\,q_m^{\pm}z}+b_m^{\pm}\,\mathrm{e}^{-\mathrm{i}\,q_m^{\pm}z}]\mathrm{J}_{n-m}\left(\frac{V_1}{\hbar\omega}\right)\\ &\quad\times\mathrm{e}^{-\mathrm{i}\,E_{zn}^{\pm}t/\hbar}\exp(\mathrm{i}\,\boldsymbol{k}_{||}\cdot\boldsymbol{\rho}-\mathrm{i}\,E_{||}^{\pm}t/\hbar),\end{aligned}\tag{8}$$

where $a_m^{\pm}$ and $b_m^{\pm}$ are constant coefficients, $\boldsymbol{\rho}(x,y)$ is a vector parallel to the plane of the potential well, $\mathrm{J}_n(x)$ is the ordinary Bessel function, and

$$q_m^{\pm}=\left[\frac{2\mu_{\pm}}{\hbar^2}\left(E_{\mathrm{F}}^{\pm}+m\hbar\omega-\frac{\hbar^2k_{||}^2}{2\mu_2}+V_0\right)\right]^{1/2},$$

with m being an integer.

Since the electrons incident to the oscillating region are scattered inelastically into an infinite number of Floquet sidebands, so the wave function outside the well can be written as the superposition of waves with all values of energy

$$\begin{aligned}\Phi_{\pm}^{(i)}(z,t)=\chi_{\pm}&\sum_{n=-\infty}^{+\infty}(c_n^{(i)\pm}\,\mathrm{e}^{\mathrm{i}\,k_{zn}^{\pm}z}+d_n^{(i)\pm}\,\mathrm{e}^{-\mathrm{i}\,k_{zn}^{\pm}z})\\ &\times\mathrm{e}^{-\mathrm{i}\,E_{zn}^{\pm}t/\hbar}\exp(\mathrm{i}\,\boldsymbol{k}_{||}\cdot\boldsymbol{\rho}-\mathrm{i}\,E_{||}^{\pm}t/\hbar),\end{aligned}\tag{9}$$

where $i=\mathrm{I},\mathrm{III}$, $E_{z0}^{\pm}+E_{\parallel}^{\pm}=E_0^{\pm}$, $E_{\parallel}^{\pm}=\hbar^2k_{\parallel}^2/2\mu_1$,

$$k_{zn}^{\pm}=\sqrt{\frac{2\mu_1}{\hbar^2}(E_{z0}^{\pm}+n\hbar\omega)},$$

and $c_n^{(i)\pm}$ and $d_n^{(i)\pm}$ are the probability amplitudes in the i-th region. The incoming and the outgoing waves (channels) of the Floquet scattering form the sidebands (or Floquet channels) with energy spacing $\hbar\omega$ according to $E_n^{\pm}=E_{\mathrm{F}}^{\pm}+n\hbar\omega$ (n is the sideband index). The mode with $E_n<0$ is an evanescent mode, and the corresponding sideband is called an evanescent sideband, because such a mode has an imaginary k_n and can not propagate.[24,25]

Using the continuities of $\Phi_{\pm}$ and $\frac{1}{\mu}\frac{\partial}{\partial z}\Phi_{\pm}$ at interfaces $z=\pm a/2$ for Eqs. (8) and (9), we obtain the scattering matrix for the single potential well[24]

$$\boldsymbol{S}_{\mathrm{total}}=\begin{pmatrix}\boldsymbol{R} & \boldsymbol{T}'\\ \boldsymbol{T} & \boldsymbol{R}'\end{pmatrix},\tag{10}$$

where $\boldsymbol{R}$ and $\boldsymbol{T}$ are matrices whose elements respectively denote the probability amplitudes of reflection and transmission for modes incident from the left (region I). For instance, the matrix element t_{nm} is the probability amplitude of transmission for an electron incident from channel m on region I to channel n on region III. The $\boldsymbol{R}'$ and $\boldsymbol{T}'$ describe the scattering process incident from the right (region III). For the model, we take $c_n^{(\mathrm{I})\pm}=\delta_{n0}$ and $d_n^{(\mathrm{III})\pm}=0$, the total electron-transmission probabilities of spin-up and spin-down components are given by

$$T^{\pm}=\sum_{n=0}^{+\infty}\frac{k_{zn}^{\pm}}{k_{z0}^{\pm}}\left|t_{n0}^{\pm}\right|^2.\tag{11}$$

The electron conductance can be obtained by means of the Landauer–Buttiker formula[26−28]

$$G^{\pm}=\frac{e^2}{h}T^{\pm}=\frac{e^2}{h}\sum_{n=0}^{+\infty}\frac{k_{zn}^{\pm}}{k_{z0}^{\pm}}\left|t_{n0}^{\pm}\right|^2.\tag{12}$$

3. Numerical results and discussion

We study numerically the scattering of a single incident wave through an oscillating quantum well and calculate the conductivity. The minimum number of sidebands needed in the sums of Eqs. (11) and (12) depends on the oscillation amplitude of the potential. According to Ref. [29], we should take $N>V_1/\hbar\omega$. In Fig. 2, we plot the conductivity $G^{\pm}$ as a function of the incident electron energy E for different incident angle θ and $V_0=300$ meV, $V_1=10$ meV, $\hbar\omega=10$ meV, $a=60$ Å. The parameters of the semiconductor heterostructure are $\gamma=187$ eV·Å^3, $\mu=0.041m_{\mathrm{e}}$ (m_{e} the mass of the free electron) for GaSb and $\gamma_1=8$ eV·Å^3, $\mu_1=0.081m_{\mathrm{e}}$ for InP according to Ref. [13]. In the actual calculation, we take $\gamma_1\approx 0$, because $\gamma\gg\gamma_1$. The interaction of the electrons with the oscillating potential leads to the photon-mediated transmission resonances. The incident electrons can emit photons

and drop to the bound states in the potential well. Similarly, the electrons in the bound states can jump to the incident channel or another Floquet channel by absorbing photons. This forms the discrete channel of scattering required by the Fano-type resonance. Once the energy difference between the incident electrons and the bound states in the well is equal to the energy of one or more photons, the transmission resonance occurs. Asymmetric Fano type resonances (involving peaks as well as dips) appear in Fig. 2. According to Eq. (7), the splitting strength of the Fano resonances between the spin-up and the spin-down states depends on the Dresselhauss coupling constant γ and the in-plane electron wave vector $\boldsymbol{k}_{||}$. The $\boldsymbol{k}_{||}$ can be tuned by changing angle θ of the incident electron. Figure 2 shows that the spin states are degenerate at $\theta = 0$, the splitting width of the Fano resonances between the spin-up and the spin-down states increases as θ increases from 0 to $\pi/2$ or as θ decreases from 0 to $-\pi/2$, and the asymmetric resonance peaks as well as the dips move toward the high energy with the increase of the incident angle θ from 0 to $\pi/2$ or with the decrease of the incident angle θ from 0 to $-\pi/2$. Because the sign of $\boldsymbol{k}_{||}$ can be changed by changing the sign of θ, the positions of the Fano resonances can be exchanged for the spin-up and the spin-down states by changing the sign of θ, as shown in Fig. 2. From Eq. (7), we can see that the in-plane electron wave vector $\boldsymbol{k}_{||}$ has the same role as the Dresselhauss coupling constant γ in the generation of the asymmetric Fano resonance peak splitting. In general, the Dresselhauss coupling constant γ is relatively more difficult to control than the in-plane electron wave vector $\boldsymbol{k}_{||}$ in experiment. This feature would allow us to achieve a simple tuning of the Fano resonance by changing angle θ of the incident electron.

Figure 3 presents the spin-up and the spin-down angle resolved conductivity spectra for different incident energy E. From Fig. 3, we can see clearly that (i) the asymmetric Fano type resonances appear, and the dips of the resonances lie on the left-hand sides of the asymmetric resonant peaks for the case $\theta \in (-\pi/2, 0]$, corresponding to the resonant case, while the dips of the resonances lie on the right-hand sides of the asym-

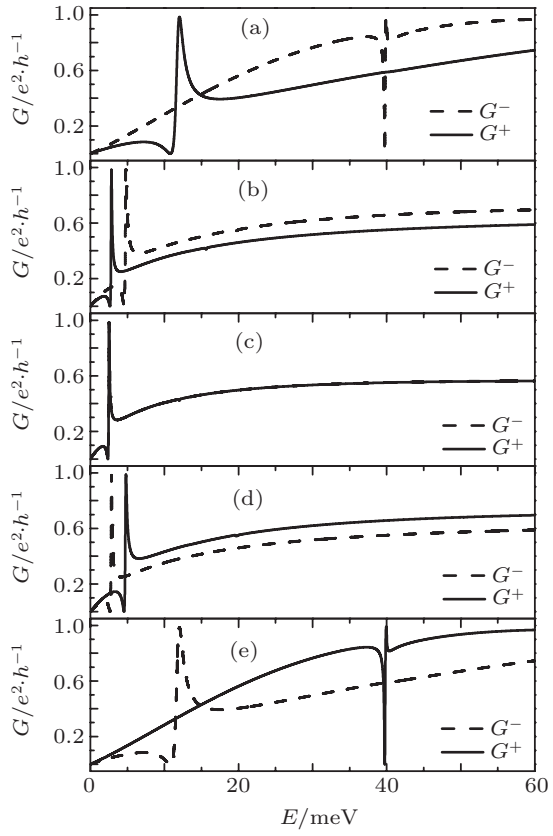


Fig. 2. Splittings of Fano-type resonances in conductivity $G^{\pm}$ at (a) $\theta = -\pi/3$, (b) $\theta = -\pi/6$, (c) $\theta = 0$, (d) $\theta = \pi/6$, and (e) $\theta = \pi/3$. The parameters are $a = 60$Å, $\hbar\omega = 10$ meV, $\mu_2 = 0.041m_e$, $\mu_1 = 0.081m_e$, $\gamma = 187$ eV·Å^3, $\gamma_1 = 0$, $V = 300$ meV, and $V_1 = 10$ meV.

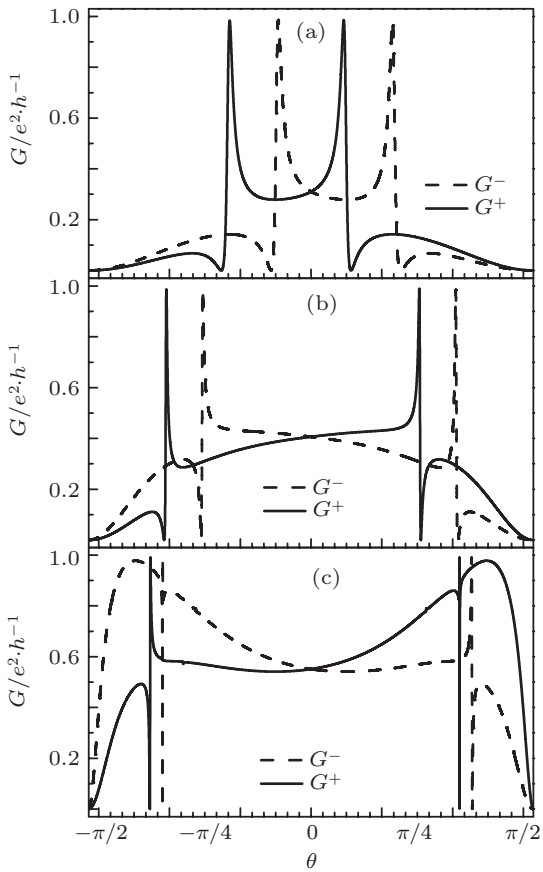


Fig. 3. Conductivity $G^{\pm}$ as a function of incident angle θ for (a) $E = 3$ meV, (b) $E = 10$ meV, and (c) $E = 40$ meV. The other parameters are given in Fig. 2

metric resonant peaks for the case $\theta \in (0, \pi/2)$, corresponding to the anti-resonant case; (ii) the asymmetric resonance peaks as well as the dips move toward the lower incident angle with the increase of the incident energy, while the asymmetric anti-resonance peaks as well as the dips move toward the higher incident angle; (iii) the splitting width of the Fano resonances between the spin-up and the spin-down states decreases as E increases.

The amplitude of the oscillating field denotes the strength of the electrons coupling to the external field. The coupling leads to a broadening of the level in the well, thus the asymmetric resonance is broadened with the increasing V_1, as shown in Fig. 4. Figure 4 shows that the asymmetric resonance peaks and dips move toward the lower incident angle with the increasing V_1, while the asymmetric anti-resonance peaks and dips move toward the higher incident angle. The results suggest a method of adjusting the line shapes and the positions of the Fano-type resonances by external parameter V_1.

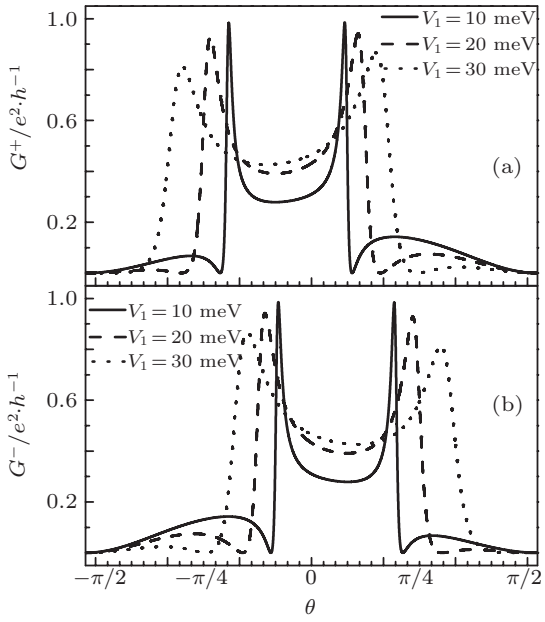


Fig. 4. Conductivities (a) G^+ and (b) G^- each as a function of incident angle θ for different V_1 with given incident energy $E = 3$ meV. The other parameters are given in Fig. 2.

The location of the asymmetric resonance peak in the incident angle parameter space depends not only on the width and the depth of the well, but also on the oscillation frequency of the external field. In Fig. 5, we plot the angle dependence of the conductivity for different applied field frequencies. As $\hbar\omega$ increases, the asymmetric resonance peaks and dips move toward the higher incident angle, while the asymmetric anti-resonance peaks and dips move toward the lower incident angle. It is apparent that controlling the location of the resonance by changing the oscillation frequency of the external field can be more easily realized in experiment than that by changing the parameters of the semiconductor heterostructure.

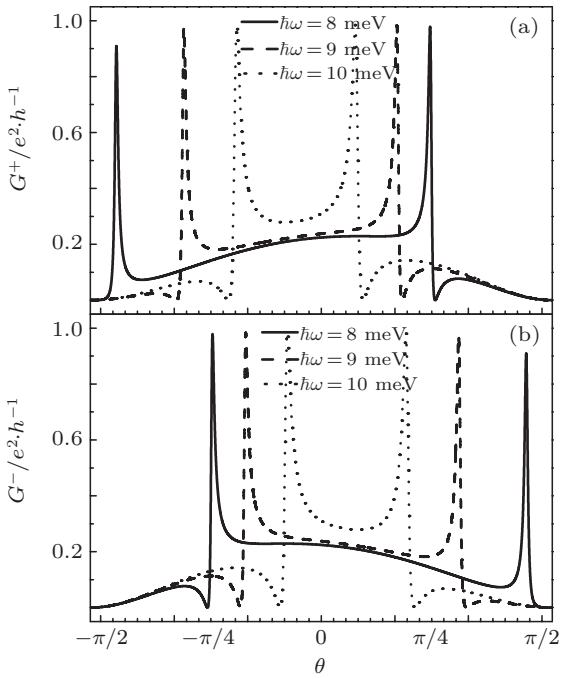


Fig. 5. Conductivity (a) G^+ and (b) G^- each as a function of incident angle θ for different frequency $\hbar\omega$ with given incident energy $E = 3$ meV. The other parameters are given in Fig. 2.

The spin-polarization dependent splitting of the Fano-type resonance peaks is advantageous to the realization of the spin current. Using the formula $P = (T^+ - T^-)/(T^+ + T^-)$, we plot the spin-polarization dependent transmission of the electrons as a function of the incident energy E for $\theta = -\pi/3$ and $\pi/3$ in Fig. 6. When $\theta = \pi/3$, the transmission current is 100% up polarized at $E = 5.19$ meV and 100% down polarized at $E = 37.13$ meV. When $\theta = -\pi/3$, the transmission current is 100% up polarized at $E = 37.13$ meV and 100% down polarized at $E = 5.19$ meV. Figure 7 shows the spin-polarization dependent transmission of electrons as a function of incident angle θ for $V_1 = 30$ meV. The transmission current is over 90% up polarized for the incident angle θ ranging from $-30\pi/100$ to $-21\pi/100$, and the transmission current is over 90% down polarized for the incident angle θ ranging from $21\pi/100$ to $30\pi/100$. The characteristics of the incident angle θ dependence of the spin-polarization current suggests that we can

exploit the Fano-type resonances as the basis for realizing a tunable spin filter and obtain a pure spin current by adjusting the external parameters, e.g., the oscillation frequency ω, the incident energy E, and the amplitude V_1 of the external field.

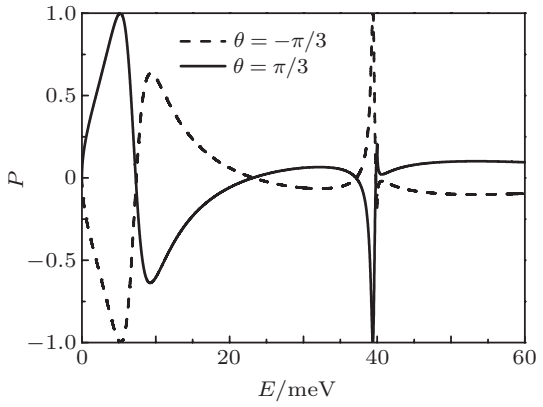


Fig. 6. Dependence of polarization of the transmission electrons on the energy of incident electron for given incident angle $\theta = -\pi/3$ and $\pi/3$ with $V_1 = 20$ meV. The other parameters are given in Fig. 2.

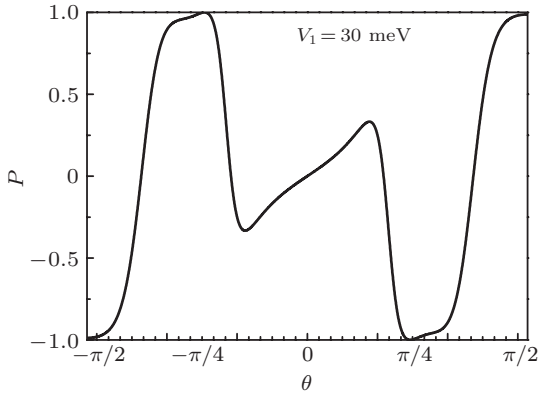


Fig. 7. Dependence of polarization of the transmission electrons on the orientation of incident electron for $V_1 = 30$ meV with given incident energy $E = 3$ meV. The other parameters are given in Fig. 2.

4. Conclusion

In summary, we have investigated theoretically the property of the electron transport through a quantum well in the semiconductor heterostructure with the spin–orbit coupling and an applied field. The numerical results demonstrate that the splitting of the asymmetric Fano-type resonance peaks due to the Dresselhaus spin–orbit coupling is highly sensitive to the direction of the incident electron. The spin polarization arising from the splitting of the Fano-type resonances exhibits an advantage for obtaining the transmission spin-polarized current. The location and the line shape of the Fano-type resonance can be controlled by changing energy E and the direction of the incident electron, oscillation frequency ω and amplitude V_1 of the external field. These interesting features not only deepen our fundamental understanding of the role of the spin–orbit coupling in solids, but also may be a very useful basis for devising tunable spin filters and realizing pure spin transmission currents.

References

[1] Tsymbal E Y, Mryasov O and LeClair P R 2003 *J. Phys.*: *Condens. Matter* **15** R109
[2] Žutić I, Fabian J and Das Sarma S 2004 *Rev. Mod. Phys.* **76** 323
[3] Schmidt G, Ferrand D, Molenkamp L W, Filip A T and van Wees B J 2000 *Phys. Rev.* B **62** R4790
[4] Rashba E I 2000 *Phys. Rev.* B **62** R16267
[5] Voskoboynikov A, Liu S S and Lee C P 1998 *Phys. Rev.* B **58** 15397
[6] Voskoboynikov A, Liu S S and Lee C P 1999 *Phys. Rev.* B **59** 12514
[7] Voskoboynikov A, Liu S S, Lee C P and Tretyak O 2000 *J. Appl. Phys.* **87** 387
[8] Ting D Z Y and Cartoixa X 2002 *Appl. Phys. Lett.* **81** 4198
[9] Koga T, Nitta J, Takayanagi H and Datta S 2002 *Phys. Rev. Lett.* **88** 126601
[10] Shang C E, Guo Y and Chen X Y 2004 *J. Appl. Phys.* **96** 3339
[11] Hall K C, Lau W H, Güdoğdu K, Flatté M E and Boggess T F 2003 *Appl. Phys. Lett.* **83** 2937
[12] Tarasenko S A, Perel' V I and Yassievich I N 2004 *Phys. Rev. Lett.* **93**, 056601
[13] Perel V I, Tarasenko S A, Yassievich I N, Ganichev S D, Belkov V V and Prettl W 2003 *Phys. Rev.* B **67** 201304(R)
[14] Glazov M M, Alekseev P S, Odnoblyudov M A, Chistyakov V M, Tarasenko S A and Yassievich I N 2005 *Phys. Rev.* B **71** 155313
[15] Zhang C X, Nie Y H and Liang J Q 2006 *Phys. Rev.* B **73** 085307
[16] Ye C Z, Zhang C X, Nie Y H and Liang 2007 *Phys. Rev.* B **76** 035345
[17] Zhang C X, Wang R, Nie Y H and Liang J Q 2008 *Chin. Phys.* B **17** 2662
[18] Zhang C X, Nie Y H and Liang J Q 2008 *Chin. Phys.* B **17** 2670
[19] Hu L Y and Zhou B 2011 *Chin. Phys.* B **20** 067201
[20] Dresselhaus G 1955 *Phys. Rev.* **100** 580
[21] Shirley J H 1965 *Phys. Rev.* **138** B979
[22] Holthaus M and Hone D 1993 *Phys. Rev.* B **47** 6499
[23] Fromherz T 1997 *Phys. Rev.* B **56** 4772
[24] Li W and Reichl L E 1999 *Phys. Rev.* B **60** 15732
[25] Bagwell P F and Lake R K 1992 *Phys. Rev.* B **46** 15329
[26] Landauer R 1989 *J. Phys.*: *Condens. Matter* **1** 8099
[27] Buttiker M 1986 *Phys. Rev. Lett.* **57** 1761
[28] Christen T and Buttiker M 1996 *Phys. Rev. Lett.* **77** 143
[29] Bulgakov E N and Sadreev A F 1996 *J. Phys.*: *Condens. Matter* **8** 8869